PACS numbers: 42.79.Qx; 42.25.Dd; 42.25.Fx
DOI: 10.1070/QE2002v032n03ABEH002172

Laser ranging of a metal target within a burning gas flame

Yu.A.Krotov

***Abstract*. The feasibility of determining the location of a metal target within a gas flame with the aid of a laser rangefinder was theoretically analysed. The effect of the gas flame composition and the combustion regime on the optical parameters of the flame, on the possibility of extracting the signal from the target against the background of the signal reflected from the flame, and also on the accuracy of determination of the target location inside the flame is taken into account.**

Keywords: *laser rangefinder, optics of flame, optics of turbid media.*

1. Introduction

The problem of removal of metal structures (derrick fragments, gas fittings, etc.) from the head of a gas well has stimulated the building of a mobile MLTK-50 industrial laser complex with a repetitively pulsed CO_2 laser with an average output power of 50 kW [1]. To direct and focus radiation from a high-power CO_2 laser, it is necessary to determine preliminary the coordinates of the elements of metal structures with a typical transverse dimension of 10 – 20 cm, which are located in a burning gas flame of about 10 m in diameter, with the aid of a laser rangefinder (LR) with an accuracy of the order of 5 – 50 cm. The minimal working distance to the flame is determined by the admissible surface density of the thermal flux from hot gas gushers with a characteristic production rate of several million cubic metres per 24 hours. For the personnel without special protective outfit and for the equipment, this distance should not be less than 100 and 50 m, respectively.

Absorption, scattering, refraction, and dispersion upon the passage of a laser radar pulse to the target and back, as well as imposition of the backscatter noise (BSN) signal reflected from the flame and the background radiation of the flame require a prior theoretical treatment of the issue. This treatment should result in the construction of the model of the flame as a medium with optical characteristics depending on the composition and combustion regime of the gas mixture.

Yu.A.Krotov M.F.Stel'makh Polyus Research & Development Institute, ul. Vvedenskogo 3, 117342 Moscow, Russia;
e-mail: mail@polyus.msk.ru, fax: 333-00-03

Received 30 January 2002
Kvantovaya Elektronika **32** (3) 243 – 246 (2002)
Translated by E.N.Ragozin

2. Model of a gas flame as an optical medium

The above-mentioned characteristic were calculated assuming that the gas flame consists of finely dispersed gas soot particles with an average radius a, a complex refractive index at a given radiation wavelength m, and a concentration N determined by the composition of the burning gas and the combustion regime. The optical parameters of the gas soot and of the gaseous components of the flame were taken into account.

The scattering and absorption coefficients and the scattering indicatrix for soot particles were calculated through the diffraction of electromagnetic field of a plane wave by spherical particles [2, 3] with a wavelength- and temperature-dependent refractive index [4 – 6]. For a hydrocarbon gas flame, the radii of soot particles lie in the 200 – 900 Å range, the average radius being of about 500 Å. If a liquid phase is present in the gusher, the droplets become carbonised and their size can achieve 1 μm [6, 7]. By assuming the soot particles to be spheres with a radius of 500 Å and refractive indices $m = 1.6 - 0.5\mathrm{i}$ and $1.7 - 0.6\mathrm{i}$ at wavelengths of 0.53 and 1.06 μm, respectively, and taking into account five terms of the expansion in terms of the parameter $2\pi a/\lambda$ in the Mie theory [2], we obtain the scattering and absorption (extinction) cross sections of a soot particle at the given wavelength.

To estimate the content of the soot in the flame, the model of underexpanded diffusion turbulent combustion of a purely gas mixture (without a liquid phase) was used [6, 8]. The concentration N of soot particles can be estimated from emission coefficient χ of the soot (the ratio between the yield of the soot and the income of carbon), which depends strongly on the fuel composition and the combustion regime for a hydrocarbon flame [4, 7]. In this case, the flow rate of gas, its composition, and the flame volume should be known. For vigorous underexpanded gas gushers, the gas flow rate Q (in m^3 per 24 hours) is estimated from the gusher height H (in metres) [8] as

$$Q(H) = 2.33 \times 10^3 H^2. \quad (1)$$

Knowing the gusher height, the emission coefficients of the soot for hydrocarbon gases, the specific density of the soot, and the average dimension of particles, we can easily estimate the concentration of soot particles. In particular, in a 20-m high methane gusher with a coefficient $\chi = 0.0015$, a soot density of 3 g cm^{-3}, and an average particle dimension of about 5×10^{-6} cm, the concentration of particles is of about 5.5×10^6 cm^{-3}, in agreement with experimental data for methane, ethylene, ethane, and acetylene combustion [5]. All these calculations can be performed for any gas

Table 1.

$\lambda/\mu m$	$a/Å$	Acetylene soot		Methane soot		Gases and vapour	
		Absorption coefficient $/10^{-2}$ cm^{-1}	Scattering coefficient $/10^{-4}$ cm^{-1}	Absorption coefficient $/10^{-4}$ cm^{-1}	Scattering coefficient $/10^{-5}$ cm^{-1}	Scattering coefficient $/10^{-8}$ cm^{-1}	Absorption coefficient $/$cm^{-1}
1.06	500	0.7	0.9	1.1	0.13	0.5	10^{-5}
	1000	1.05	1	1.5	1		
0.53	500	1.9	10	2.75	1.4	8	Svan bands
	1000	2.3	70	3.25	10		

mixture of known composition taking into account that the emission coefficient of the soot for ethane is the same as for methane, while for ethylene, propane, and butane, it is three times that for ethane, and for acetylene it is 70 times higher [5] than for ethane.

The signal attenuation after the double passage through a ten-metre flame caused by scattering and absorption by the soot was calculated using the above results. In particular, the signal is attenuated by an order of magnitude in the methane flame, whereas the signal is attenuated by 12 orders of magnitude in the acetylene flame. This points up to the fundamental significance of the knowledge of the gas composition of the burning gusher.

In addition to the soot, account was also taken of the contribution of gaseous components of the flame to the scattering and absorption. The Rayleigh scattering by gas density fluctuation and the absorption of gas flame component were calculated on the basis of the standard atmospheric model, replacing oxygen by combustion products in the percentage composition of the atmosphere and taking into account the high temperature of the flame: $T = 1500 - 2000$ K [9–11]. The gaseous medium of a hydrocarbon flame differs from the standard atmosphere in that oxygen is almost entirely absent and is replaced by combustion products: water vapour, CO_2, CO, OH, and unburned hydrocarbons. Note that the volume moisture content of a hydrocarbon flame is typically an order of magnitude higher that that of a standard atmosphere and may achieve several tens of percent when the burning mixture contains a large amount of hydrogen [12]. The elevated flame humidity and temperature cause additional Rayleigh scattering and absorption (especially by water molecules at 1.06-μm range).

All calculations were performed for two wavelengths (1.06 and 0.53 μm) and two characteristic average dimensions of soot particles (500 and 1000 Å), and the soot concentration was calculated for two hydrocarbon gases extreme as regards soot production: methane – the one with the lowest soot release, and acetylene – the one with the highest. The main results of calculations of the coefficients of absorption and scattering by solid (soot) and gaseous flame components are given in Table 1.

By comparing the scattering and absorption data for soot aerosols and gaseous flame components, note that the water vapour absorption coefficient at 1.06 μm is significantly higher than the Rayleigh scattering coefficient, and the coefficients of absorption and scattering by the soot will exceed the water vapour absorption coefficient for a concentration of soot particles of $10^6 - 10^7$ cm^{-3} and over. By going over to a wavelength of 0.53 μm we almost get rid of the water vapour absorption (in this case, however, account should be taken of the absorption by C_2 radicals – the Svan bands), but the Rayleigh scattering coefficient increases 16-fold, the absorption coefficient of the soot rises two-fold, the scattering coefficient of the soot rises by an order of magnitude. In this case, the Rayleigh scattering can be neglected when the concentration of soot particles is higher than 10^3 cm^{-3}.

3. Estimate of the intensity of the BSN signal from a gas flame and its comparison with the background flame intensity

We write down the well-known expression for the power of the signal recorded with a lidar, which arises from the scattering of a short optical pulse in a turbid medium:

$$P_{\mathrm{brs}} = P_0 \frac{S}{2\pi(r+z)^2} \frac{c}{n} \tau \alpha_{\mathrm{s}}(z) f(\pi, z) \times \exp\left[-2\int_0^{r+z} \varepsilon(x)\mathrm{d}x\right], \quad (2)$$

where P_0 is the outgoing radiation power; S is the detector area; $c/n\tau$ is the pulse length in the medium; z is the distance to the scattering volume in the flame; $\alpha_{\mathrm{s}}(z)$ is the scattering coefficient at the point z; $f(\pi, z)$ is the backward scattering indicatrix; r is the distance to the flame; and $\varepsilon(z)$ is the extinction coefficient at the point z. Table 2 shows the P_{brs}/P_0 ratio calculated for two wavelengths, two distances to the flame (100 and 50 m), and two gases (methane and acetylene) assuming the Rayleigh scattering indicatrix and a pulse duration of the order of 10^{-8} s.

Table 2.

$\lambda/\mu m$	Methane		Acetylene	
	$H = 100$ m	$H = 50$ m	$H = 100$ m	$H = 50$ m
1.06	0.25×10^{-11}	10^{-11}	1.5×10^{-10}	6×10^{-10}
0.53	0.3×10^{-10}	1.2×10^{-10}	10^{-10}	4×10^{-10}

When estimating the background flame intensity at the LR photodetector, the flame was assumed to be a blackbody with a temperature T, which is usually lying between 1400 and 2000 K for a hydrocarbon flame. For a flame temperature T = 1400 K, a change-over from $\lambda = 1.06$ μm to $\lambda = 0.53$ μm reduces the background flame power by a factor of 500, whereas for $T = 2000$ K by only a factor of 30.

The total power of background flame radiation incident on the photodetector objective with an area of 40 cm^2 and passing through an interference light filter with a 20-nm wide transmission band on bringing into coincidence the detector and transmitter apertures is proportional to the area of the laser spot on the flame. For an angular beam divergence of about 2′, this spot does not exceed 5 cm in diameter at a distance of 100 m. Depending on the flame temperature, the background power is in the 8×10^{-8}–

1.5×10^{-6} W range for a wavelength of 1.06 μm and in the $1.7 \times 10^{-10} - 5.8 \times 10^{-8}$ W range for a wavelength of 0.53 μm. For an outgoing LR radiation power of the order of 2×10^{6} W (a pulse energy of 28 mJ at a wavelength of 1.06 μm, a half-height pulse duration of 12 ns), the BSN signal exceeds the flame background signal by at least 2–3 orders of magnitude in intensity. The issue of radiation capacity of the flame is treated in greater detail elsewhere [13–15].

The problem of laser pulse reflection from the gas flame was solved by numerical simulation in the single- and multiple-scattering approximations using the Green function for the transient equation of electromagnetic radiation transfer in turbid media [16–18]. The optical parameters of the flame were assumed transversely uniform. The problem was solved for two different laser pulse shapes: symmetric (Gaussian) and steep-edged (exponential). For a methane flame, in which the characteristic photon scattering time exceeds the radar pulse duration by more than an order of magnitude, the problem was solved in the single-scattering approximation. For an acetylene flame, wherein the photon collision time is shorter than or of the order of the pulse duration, the Green function of the transfer equation for multiple scattering was used [16].

Figs 1 and 2 show the results obtained. Noteworthy is the fundamentally different behaviour of the BSN for weakly and strongly scattering media: in the weakly scattering medium there occurs a characteristic prolongation of the trailing pulse edge, while in the strongly scattering one the pulse shape is reproduced.

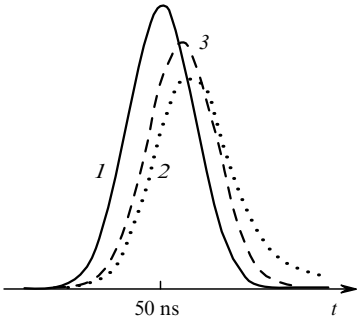

Figure 1. Deformation of a Gaussian laser pulse (*1*) upon reflection from a weakly scattering medium – a methane flame (*2*) and from a strongly scattering medium – an acetylene flame (*3*).

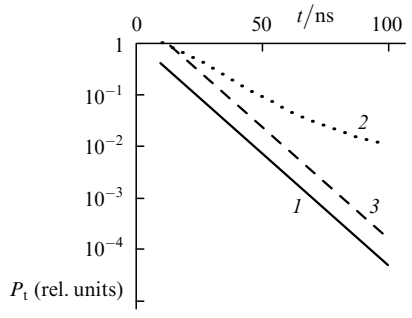

Figure 2. Deformation of an exponentially decaying laser pulse (*1*) upon reflection from the weakly scattering medium – a methane flame (*2*) and from the strongly scattering medium – an acetylene flame (*3*).

4. Signal reflected from the target and imposition of the BSN signal

The power of a signal reflected from the target with a diffuse reflectance R residing in the flame at a depth z is, assuming the radiator optics to match the detector optics of area S, given by the expression

$$P_t = P_0 \frac{SRK}{\pi(r+z)^2} \exp(-2\varepsilon_a r) \exp(-2\varepsilon_f z), \tag{3}$$

where K is equal to either unity or the ratio between the transverse dimensions of the target and the beam, d_t and d_λ; $\varepsilon_{a,f}$ are the extinction coefficients for the atmosphere and the flame. The diffuse reflectances of a metal covered with a soot layer no thinner than the wavelength in the soot are easy to calculate [5, 9] and are equal to 0.111 and 0.087 at wavelengths of 1.06 and 0.53 μm, respectively.

We determine the ratio between the target-generated signal and the BSN power for a confocal radiator–detector geometry, different positions of the target inside the flame, different transverse target–beam dimension ratios, and the two flames (methane and acetylene) extreme in soot release. The target-produced-to-BSN signal ratio is $\eta = P_t/P_{brs}$.

(1) The target intercepts the beam completely ($K = 1$), the damping is low ($1/\varepsilon \gg D$, where D is the transverse flame dimension), the target is located at an arbitrary depth $z < D$ in the flame, and $z \gtrless c\tau/n$:

$$\eta_1 = 2R/[z\alpha_s f(\pi)]\,. \tag{4}$$

(2) The target intercepts the beam partially [$K = (d_t/d_\lambda)^{(1\div 2)}$], the damping is low, the target is located at an arbitrary depth in the flame:

$$\eta_2 = \frac{2RK}{[z + (D-z)K]\alpha_s f(\pi)}. \tag{5}$$

(3) The damping is strong, the target is located deep in the flame ($L = 1/\varepsilon < c\tau/n \ll z < D$):

$$\eta_3 = \frac{2RK\exp(-2\varepsilon z)}{L\alpha_s f(\pi)\exp(-2\varepsilon L)}. \tag{6}$$

(4) The damping in the flame is strong, the target is located not deep in the flame ($z < 1/\varepsilon < c\tau/n < D$):

$$\eta_4 = \frac{2RK}{[z + (L-z)K]\alpha_s f(\pi)}. \tag{7}$$

For a methane flame in the first case, for a wavelength of 1.06 μm the quantity $\eta_1 = 8 \times 10^5$ cm z^{-1} and may vary within the $10^6 - 10^3$ range, while for a wavelength of 0.53 μm $\eta_1 = 8 \times 10^4$ cm z^{-1} and may vary within the $10^5 - 10^2$ range. For an acetylene flame in the third case when z is varied from 100 to 1000 cm, for a wavelength of 1.06 μm the quantity $\eta_3 = 80\exp[-(2 \times 10^{-2}\ \text{cm}^{-1})z]$ and varies in the $10^2 - 10^{-7}$ range, while for a wavelength of 0.53 μm $\eta_3 = 1600\exp[-(4 \times 10^{-2}\ \text{cm}^{-1})z]$ and varies in the $10 - 10^{-14}$ range.

In the computer simulation it has been possible to take into account the effect of superposition of target-produced and BSN signals on the position of their peaks and, hence, the measurement accuracy of the distance to the target for different laser pulse shapes, different target-produced-to-BSN signal amplitude ratios, and different positions of the target inside the flame. In particular, for a Gaussian pulse and a 1/1 amplitude ratio, the peaks are well resolved when they are spaced at more than a pulse length τ. In this case,

they draw most close together when the centre-to-centre distance of the pulses is in the $(2 \div 3)\tau$ range. In our case, the shift is highest for $t_1 - t_2 = 2.25\tau$ and amounts to $(1/3 \div 1/5)\tau$ for signals of equal amplitude. For $\tau = (5 \div 6) \times 10^{-9}$ s this is responsible for a distance measurement error of about 50 – 30 cm.

For a Gaussian pulse, a BSN-to-target-produced signal amplitude ratio of 10/1, and an interpulse distance below three halfwidths, the second peak is not resolved and the superposition reduces to the prolongation of the corresponding front of the higher-power pulse. And it is only when the pulses are spaced at more than 3.5τ that the peaks of the Gaussian pulses are clearly differentiated, no peak shifts being observed in this case. For a pulse of exponential shape and amplitude ratios of 1/1 an 10/1, the signals are easily distinguishable even for peak-to-peak distances equal to 1/3 of the pulse duration. In this case, the signal resulting from the superposition of the target-produced and BSN signals exhibits no significant peak shifts even when the amplitude ratio is 1/1.

5. Azimuth errors

The possible error in the determination of the target position in a gas flame is due to regular and random refraction of the laser pulse on its path to the target. The regular refraction is determined by the refractive index gradients in the atmosphere and the flame. It depends primarily on the temperature, humidity, and pressure gradients in the atmosphere and on the gradients of the density of combustion products and the temperature in the flame. The random refraction arises from the motion of inhomogeneous optical medium due to turbulence. It seems likely that its contribution can be neglected because of the rather low frequencies of these processes and short optical path lengths in the atmosphere and the flame for laser pulse lengths of less than 10^{-8} s.

The regular atmospheric refraction was estimated using a standard dependence of the refractive index of the atmosphere on the radiation wavelength and the temperature and humidity gradients [10]. For typical drops of temperature and humidity (their gradients are opposite in sign) across LR – flame paths of the order of 100 m long and a radiation wavelength of 1.06 μm, the refraction angle amounts to $\sim 4 \times 10^{-5}$ rad as a maximum. This is an order of magnitude lower than the divergence angle of the laser beam, which provides a spot with a lateral dimension of no greater than 5 cm at a distance of 100 m.

As for the regular refraction in the flame due to the nonuniformities of the flame parameters over the transverse flame section, the estimate gives the azimuthal error of determination of the target position of the order of 10 – 15 cm based on the model of underexpanded diffusion turbulent combustion of a purely gaseous hydrocarbon mixture [6, 7] for a radiation wavelength of 1.06 μm and a gusher with a production rate of no less than 10^6 m^3 per 24 hours, and a flame diameter of 10 m. In the case of the second harmonic at 0.53 μm, the azimuthal error is larger.

6. Conclusions

The theoretical analysis of absorption and scattering of a laser pulse in a gas flame has revealed the dependence of the absorption and scattering coefficients on the composition and combustion regime of a real gas well. In specific cases, the BSN signal can exceed the target-produced signal by many orders of magnitude, making the detection and measurement of the coordinates of the target inside the flame virtually impossible.

The target-produced signal can be easily detected when it is no weaker than one tenth of the BSN signal and the peak-to-peak distance of the pulses exceeds the laser pulse halfwidth. In this case, the measurement accuracy of the distance to the target lowers, especially so for symmetrically shaped pulses with gently sloping edges. The change-over to the second harmonic ($\lambda = 0.53$ μm) in a LR impairs the situation in the majority of cases (with the exception of the flame-produced background).

In connection with the foregoing, the derivation of experimental data on the laser pulse scattering and absorption in real gas flames is a topical problem. This would set the stage for the formulation of several inverse problems in scattering, the problem of reconstructing optical flame parameters from the characteristics of reflected signal in particular. As for the theory of the problem, account should supposedly be taken of both the large-scale flame inhomogeneities due to the turbulent nature of combustion and of the nonuniformities of the optical characteristics of the flame over its lateral section arising from the gradients of temperature, soot concentration, etc. in various combustion modes. The prospect of using polarised radiation in this problem should also be examined.

Acknowledgements. The author is grateful to V.A.Pashkov and Yu.V.Abazadze for fruitful discussions on the paper and financial support of the work.

References

1. Krasyukov A.G. *Lazer-Inform*, **210 – 211** (3 – 4), 4 (2001).
2. Mie G. *Annal. der Phys.*, **25**, 377 (1908).
3. Born M., Wolf E. *Principles of Optics* (Oxford: Pergamon Press, 1969).
4. *Encyclopedia of Industrial Chemical Analysis* (London: Interscience Publ., 1967) Vol. 2, p. 11.
5. Levashenko G.I., Simon'kov V.V. *Fiz. Goren. Vzryv.*, **31**, 70 (1995).
6. Thring M.W., et al. *Combustion and Flame*, **22**, 503 (1974).
7. Becker H.A., Liany D. *Combustion and Flame*, **44**, 305 (1982).
8. Akhmetov D.G. *Fiz. Goreniya Vzryva*, **30** (6), 25 (1994).
9. Landau L.D., Lifshits E.M., Pitaevskii L.P. *Electrodynamics of Continuous Media* (Oxford: Pergamon Press, 1984; Moscow: Nauka, 1982).
10. Zuev V.E. *Rasprostranenie lazernogo izlucheniya v atmosfere* (Propagation of Laser Radiation in the Atmosphere) (Moscow: Radio i Svyaz', 1981).
11. Zuev V.E., Kabanov M.V. *Optika Atmosfernogo Aerozolya, Ser. 'Sovremennye Problemy Atmosfernoi Optiki'* (Optics of Atmospheric Aerosol, Modern Problems of Atmospheric Optics) (Leningrad: Gidrometeoizdat, 1987) Vol. 4.
12. Poluektov N.S. *Metody analiza po fotometrii plameni* (Techniques of Flame Photometry Analysis) (Moscow: Khimiya, 1967).
13. De Faveri D.M., et al. *Hydrocarbon Processing*, **64** (5), 89 (1985).
14. Coppale A., Vervisch P. *Combustion and Flame*, **49**, 101 (1983).
15. Howarth C.R., et al. *Proc. Intern. Heat Transfer Conf. AICRE* (Chicago, 1966) Vol.5, p. 122.
16. Zege E.P., Ivanov A.P., Katsev I.L. *Perenos izobrazheniya v rasseivayushchei srede* (Image Transfer in a Scattering Medium) (Minsk: Nauka i Tekhnika, 1985).
17. Skrelin A.L., Ivanov A.P., Kalinin I.I. *Fiz. Atm. Okeana.*, **6**, 889 (1970).
18. Katsev I.L., Ivanov A.P. *Vestn. Akad. Nauk BSSR. Ser. Fiz. Mat.* (4), 102 (1968).